Proceedings of the International Conference on New Trends in Transport Phenomena
Ottawa, Ontario, Canada, May 1-2 2014
Paper No. 82

Process Optimization for the Electrospinning of Polycaprolactone Nanofibers Using Non-halogenated Solvents

Siavash Sarabi-Maneji, Jennifer Scott and Danny J.Y.S. Pagé
Royal Military College of Canada, Department of Chemistry and Chemical Engineering
Kingston, Ontario, Canada, K7K 7B4
siavash.sarabi-mianeji@rmc.ca; jennifer.scott@rmc.ca; page-d@rmc.ca

Abstract- In this paper, polycaprolactone nanofibres were processed by electrospinning using a 3:1 ratio of tetrahydrofuran to methanol as solvent. The solvent choice was motivated by the possibility of greener alternatives to the halogenated compounds most often used for electrospinning. This paper presents the morphologies and fiber diameters resulting from the electrospinning of polycaprolactone solutions at room temperature under various conditions. The material morphology was characterized using scanning electron microscopy and a measuring software. The process was optimized for smaller fibers with a narrower fiber diameter distribution by studying parameters such as polymer concentration, applied voltage, the tip to collector distance, and the solution flow rate. The experimental results were modelled using terminal jet diameter theory used in several referenced work. The theory behind this model was used to analyse the experimental observations made in the current paper. Process parameters were optimal for a 20% polycaprolactone concentration spun at a flow rate of 0.5 mL/h, with a tip to collector distance of 15 cm and an applied voltage of 8 kV. Fibers spun under these conditions displayed diameters of 546 ± 173 nm.

***Keywords*:** Electrospinning, nanofibers, polycaprolactone, methanol, tetrahydrofuran.

1. Introduction

The emergence of nanomaterials over the last few decades has provided enormous potential for the production of increasingly lighter, stronger and smaller system components for high-tech applications. Nanomaterials come in various shapes and compositions and are characterized by a high surface area, often possessing distinctive properties from their macroscale counterparts. Polymeric nanofibers with diameters in the nanoscale range support numerous applications, such as scaffolds for tissue engineering, sensoring devices and high strength structures for use in infrastructure or transport platforms (Baji et al., 2010; Subbiah et al., 2005). In particular, the ability to produce nanofibers of polycaprolactone (PCL) is of great interest due to its biodegradability and long standing use in biomedical applications.

While mechanical conventional spinning methods are unable to produce fibers with diameters less than two microns (Dzenis, 2004), polymeric nanofibers can be processed by techniques such as drawing (Nain et al., 2006), template synthesis (Huczko, 2000) and electrospinning (Baji et al., 2010; Subbiah et al., 2005). The drawing technique uses a sharp tip to draw a polymer solution from its deposited droplet, producing single, solidified nanofibers due to the fast evaporation of the solvent. Template synthesis is a technique which uses a nanoporous membrane as a template for the growth of nanofibers. In contrast, electrospinning forms nanofibers by drawing a polymer solution using an electric field.

Electrospinning stands out as a transport phenomenon by using a high strength electromagnetic field to propel and transform matter in space. The process establishes a high voltage between the needle of a solution delivery system, such as a syringe pump, and a metallic target as the collector. During the procedure, the polymer solution is charged at the needle and flows out as a continuous jet. During its trajectory, the jet becomes considerably elongated, bent in a spiral shape and dried in space until it reaches the collector (Reneker et al., 2000). If the solution and processing conditions are appropriate, a

continuous nanofilament is produced. A typical electrospinning set-up, such as the one shown in Fig.1, has been used for the work presented in this paper.

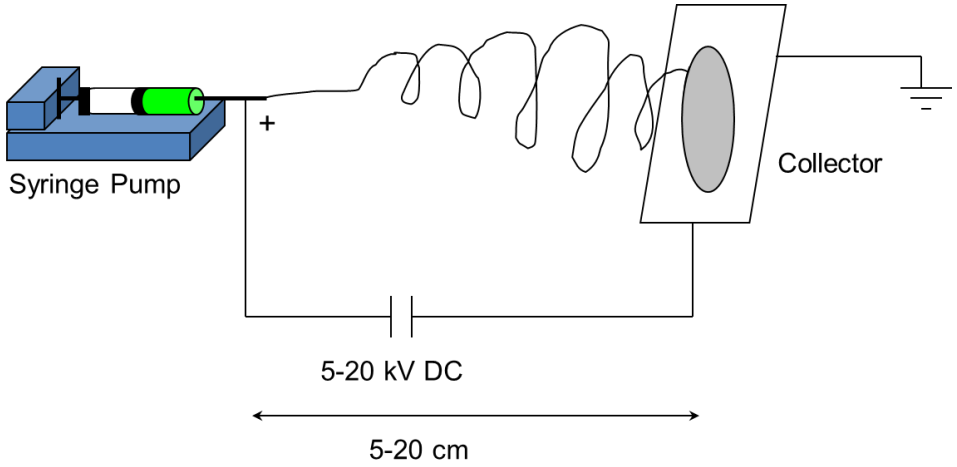

Fig. 1. Typical experimental set-up used for the electrospinning of polymer solution.

Although the last decade has seen a considerable increase in the interest towards electrospinning from researchers, the first occurrence of electrospinning actually dates back to 1914 when John Zeleny reported the behavior of conductive liquid droplets in the end of metallic tubes in the presence of an electrostatic force (Nain et al., 2006). Several years later, Anton Formhals (1934) contributed to the development of electrospinning and published several patents on the technology. Sir Geoffrey Ingram Taylor (1969) improved upon the theoretical aspects of electrospinning parameters, specifically the mathematical modelling and experimental measurements of the changing shape of a conductive liquid droplet (called the Taylor cone) above a critical electromagnetic field.

In recent years, models have been developed in order to optimize the intricate physical processes of electrospinning (Reneker et al., 2000; Fridrikh et al., 2003; Thompson et al., 2007; Reneker et al., 2007). These models have led to progress in making electrospinning a more scalable process for industrial applications (Luo et al., 2012a). The model by Fridrikh et al. (2003) was used to fit the results presented in this paper and is therefore shown below in Equation 1. The model presents the terminal diameter of the whipping jet, h_t, once equilibrium is reached between the surface tension of the solution forming the jet and the surface charge repulsion generated on the jet's surface as it travels in the high electromagnetic field.

$$h_t = \left(\gamma\varepsilon\frac{Q^2}{I^2}\frac{2}{\pi(2\ln\chi-3)}\right)^{1/3} \tag{1}$$

Other parameters found in this equation are the surface tension γ, the dielectric constant of the surroundings ε, the volumetric flow rate Q, the current I and the ratio between contour length of the jet over the radius of curvature of whipping χ. In another version of Equation 1 (Baji et al., 2010), h_t is replaced by D, the spun fiber diameter, and χ is replaced by l/d, the ratio of the initial jet length, prior to whipping, over the internal diameter of the nozzle.

Electrospinning can be performed from a polymer melt, but it more often involves a solvent (Reneker et al., 2007). Although halogenated solvents are very effective for preparing solutions of a wide variety of polymers (Zoppe et al., 2009; Subbiah et al., 2005), they are unfortunately among those that pose the highest safety risk to human health and are also among the hardest to dispose of (Valavanidis and Vlachogianni, 2012). Weighing solubility and environmental concerns for electrospinning, or any other process, on an industrial scale can be challenging. Recent work on the solubility of

polymethylsilsesquioxane (PMSQ) (Luo et al., 2010) and PCL (Luo et al., 2012b) in various solvents, and the electrospinnability of the resulting solutions, shed some light on selecting an effective solvent system for the processing of polymer filaments by electrospinning. Findings suggest that higher solubilities do not necessarily produce spinnable solutions, but rather solvent systems combining a solvent and a non-solvent produce better spinning results (Luo et al., 2010). In fact, choosing a non-solvent with a higher dielectric constant produced the best electrospinning results (Luo et al., 2012b). Based on the aforementioned work, tetrahydrofuran and methanol were selected as solvent and high dielectric non-solvent, respectively, for the electrospinning of PCL presented in this paper. The choice of these solvents was also motivated by the fact that they are not halogenated and therefore greener choices.

2. Methodology

2. 1. Materials

Polycaprolactone (PCL) is a biodegradable polyester with a low melting point (around 60 ^{o}C) and a T_g of -60 ^{o}C. A Capa 6500 grade was obtained from Perstorp with a mean MW of 50 000. PCL was dissolved in a 3:1 solution of Tetrahydrofuran (THF) to Methanol (MeOH), both obtained from Caledon Labs, with respective purities of 99% and 99.8%. Solutions were prepared with the desired concentrations in w/v% by mixing the components and stirring for 24 hours at room temperature using a magnetic stir plate. Resulting solutions were then used in the electrospinning process.

2. 2. Electrospinning

A typical electrospinning set-up was used, such as the one shown in Fig.1. A high voltage power supply (PS375/+20KV, Stanford research system) was used to generate a DC voltage from 5kV to 18 kV. A 5 mL glass syringe with a 18G flat tip needle (inside diameter of 0.838 mm) was used as a sample container feeder. A rotating drum covered with aluminum foil was used as a collector. A programmable syringe pump (Fisher Scientific) maintained the desired flow rate throughout each trial. The positive electrode from the power supply was attached to the needle and the negative electrode was attached to the grounded collector.

2. 3. Scanning Electron Microscopy

A Scanning Electron Microscope (SEM), model XL 30 from Philips (USA), was used to characterize spun fibers. The software Image J was then used to measure the fiber diameter of at least 35 fibers in each of the samples analyzed. The standard deviation (SD) on fiber diameter is reported as error bars in each of the Fig. 3 to 6 and represents 105 measurements over three samples (3 x 35).

3. Results and Discussion

The following figures present the morphologies and fiber diameters resulting from the electrospinning of PCL solutions of THF-MeOH in a 3:1 ratio at room temperature under various conditions. The process was optimized towards smaller, more homogeneous sample diameters by studying parameters such as PCL concentration, applied voltage, tip to collector distance (TCD) and flow rate. The experimental results were modelled using Equation 1. The χ value used in the model was estimated to be 12 using the *l/d* definition.

The effect of a change in the concentration of PCL in the polymer solution is shown in Fig. 2 and 3. PCL concentrations in the processing solutions were varied from 5% to 35% at a flow rate of 1 mL/h, a tip to collector distance of 10 cm and an applied voltage of 10 kV. Concentrations of 5% and 8% produced nanofibers with a morphology primarily composed of polymer beads with small amounts of fibers. PCL concentrations of 12% and 15% produced fibers with a consistent morphology containing beads, like the one shown on the left hand side of Fig.2. At 18% PCL, the number of beads significantly decreased but were still visible. For PCL concentrations of 20% and greater, a consistent morphology of fibers with an absence of beads was obtained, as shown on the right-hand side of Fig.2. Mass balance calculations revealed that over 97% of the PCL from the solution was recovered on the collector.

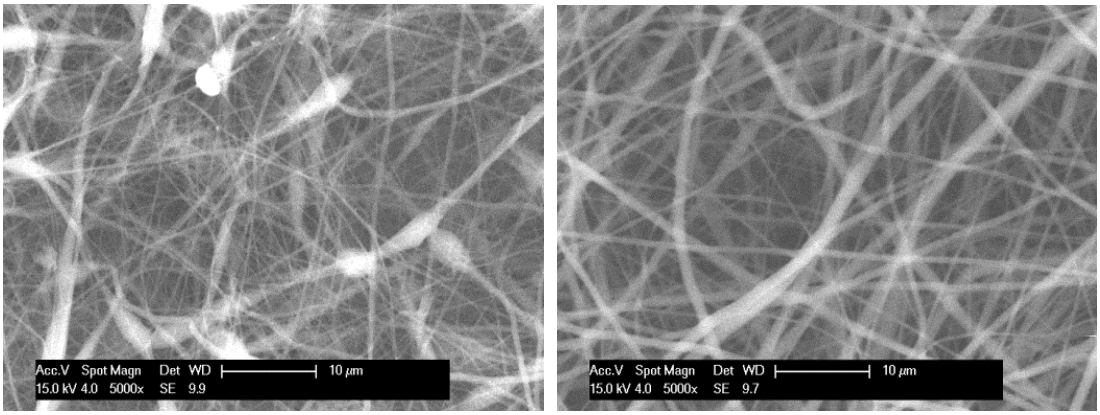

Fig. 2. SEM micrographs for fibers spun from solutions of 15% PCL (left) and 20% (right). Other processing conditions included a flow rate of 1 mL/h, a tip to collector distance of 10 cm and a voltage of 10 kV.

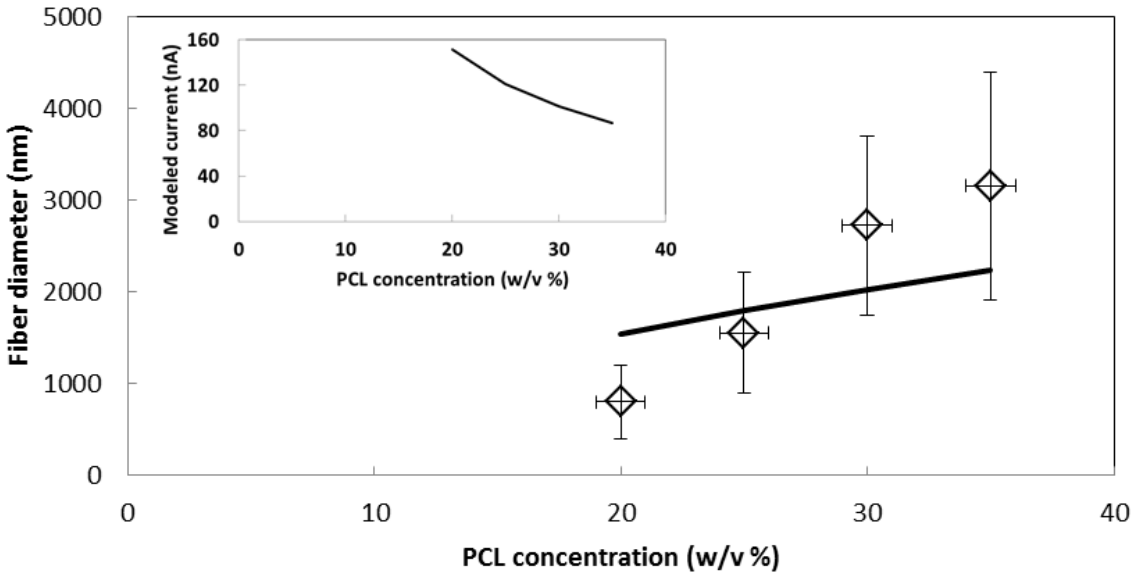

Fig. 3. Fiber diameter as a function of PCL concentration (symbols) at a distance of 10 cm and voltage of 10 kV. Fit to the terminal jet diameter theory (curve) was obtained by modelling the current as a function of $I = f(1/[PCL])$, as shown in the inset. Other model parameters included γ=29.6 dyn/cm, $\varepsilon = 1$, $Q = 1$ mL/h and $\chi = 12$.

The results of varying PCL concentration are shown in Fig.3, where the measured fiber diameter is shown to increase as a function of PCL concentration. Only those PCL concentrations that produced fibers and no beads are shown. The standard deviation of the diameter, represented by the vertical error bars, also increases with the PCL concentration, with the 20% PCL concentration producing the smallest fibers at 800 nm and also the fibers with the narrowest size distribution at 400 nm. In order to attempt a fit of the model represented by Equation 1 to the experimental results and represent the trend of increasing diameter with increasing concentration, the current must decrease as a function of concentration, as shown in the inset. The dielectric constants of MeOH, THF and PCL are 32.7, 7.58 and about 3, respectively, resulting in MeOH being the most conductive medium with a conductivity of 4 μS/cm. As the PCL concentration increases, the portion of MeOH in the jet decreases, resulting in a decrease in the conductivity of the jet and a consequent decrease in the current passing through. It should be noted that the electrical current measured during electrospinning was barely measurable, being just below 1 μA, which is higher than the ~100 nA current values used to fit the model. The aforementioned

observation can be explained by the volatility of THF and MeOH, with boiling points of 66°C and 64.6°C, respectively, resulting in evaporation of the solvent during the process, as indicated by Fridrikh et al. (2003). Although some of the solvent may no longer be part of the jet during processing, MeOH molecules are still trapped in the electromagnetic field and may be responsible for a significant portion of the observed current.

The effect of applied voltage on the diameter of the resulting fiber is presented in Fig.4, displaying an increase in the fiber diameter with increasing voltage. In order to fit the model represented by Equation 1 to the experimental results, the current must decrease as a function of the applied voltage, as shown on the inset of Fig.4. As the applied voltage increases more material is drawn into the electrical field leading to a larger jet diameter. In accordance with the terminal jet diameter theory, charge repulsion would see charges accumulating near the surface of the jet (Fridrikh et al., 2003). Since a larger jet diameter would result in a lower aspect ratio, less surface area per volume of material travelling in the jet is available for the passage of current. The fit of the model deviates from the experimental results at low voltage. The model is primarily focused on the electrospinning process and does not capture the competition between laminar flow generated by the pump through the nozzle and the jet flow generated by the electromagnetic field at low voltage.

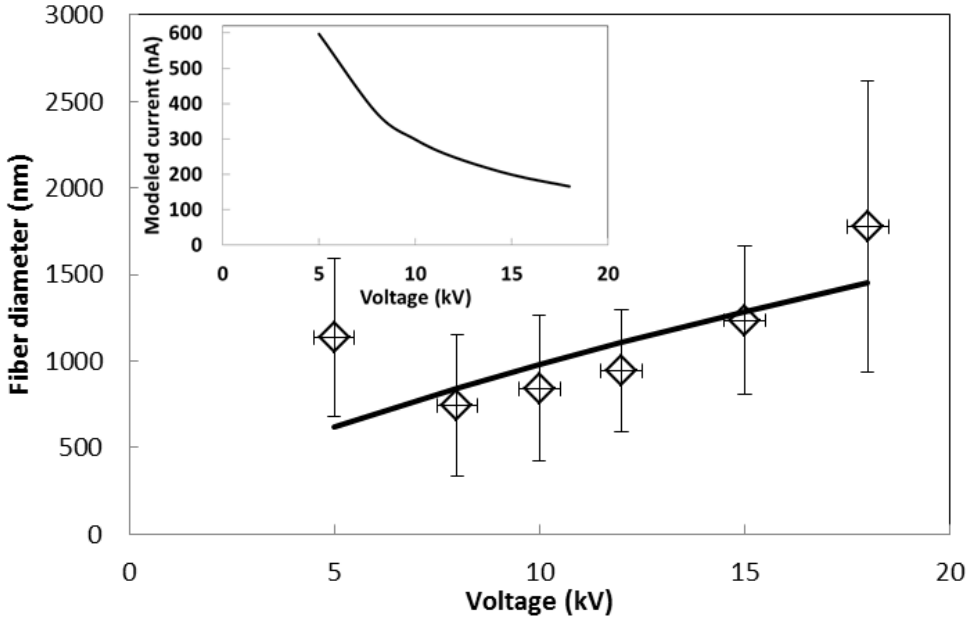

Fig. 4. Fiber diameter as a function of the applied voltage (symbols) at a distance of 10 cm and a [PCL] of 20%. Fit to the terminal jet diameter theory (curve) was obtained by modelling the current as a function of $I = f(1/V)$ as shown on the inset. Other model parameters used were γ=29.6 dyn/cm, $\varepsilon = 1$, $Q = 1$ mL/h and $\chi = 12$.

As the tip to collector distance (TCD) is increased, the measured fiber diameter decreases, as shown in Fig.5. As the distance increases, the jet becomes more stretched, thereby reducing the jet diameter. The model represented by Equation 1 does fit the experimental results better than the parameters studied in the previous figures. In order to follow the trend and have the diameter decrease with distance, the current must increase as a function of the distance, as shown on the inset of Fig.5. The increase of the current with distance is consistent with the corresponding decrease in jet diameter and consequent increase in the aspect ratio (as discussed above for Fig.4). The smallest fiber diameter observed with the narrowest size distribution was processed at a distance of 15 cm, resulting in a fiber diameter of 546 ± 173 nm.

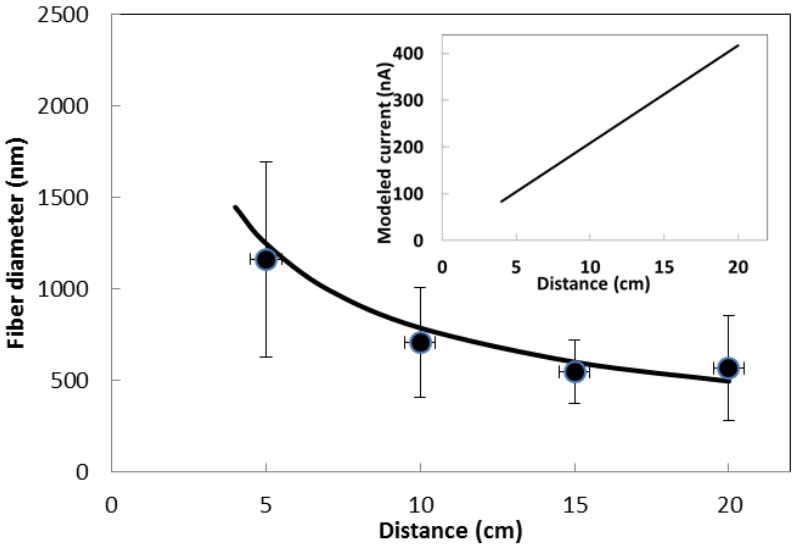

Fig. 5. Fiber diameter as a function of tip to collector distance (symbols) at a voltage of 8 kV and a [PCL] of 20%. Fit to the terminal jet diameter theory (curve) was obtained by modelling the current as a linear relationship with tip to collector distance, $I = f(\text{TCD})$, as shown on the inset. Other model parameters used were $\gamma = 29.6$ dyn/cm, $\varepsilon = 1$, $Q = 0.5$ mL/h and $\chi = 12$.

When the flow rate of the polymer solution is increased, the fiber diameter also increases, as shown in Fig 6. Modelling the experimental results using Equation 1 leaves much to be desired. The fiber diameter obtained at 0.2 mL/h was much higher than the trend suggested by the model. The vertical error bar associated with that point and the SEM micrograph on the right side of Fig.6 both indicate a large variation in diameter size. The difference in fiber size points towards flow variations possibly caused by occasional deformations resulting from the competition between the laminar flow coming out of the nozzle being too slow for the pull flow generated by the electromagnetic field. The model represented by Equation 1 was based on conditions dominated by forces generated by the electromagnetic field which may not apply to the aforementioned observations made at a flow rate of 0.2 mL/h. In addition, the model was calculated at constant current. However, since the flow rate increases and generates a larger fiber diameter it would be expected to see the current decrease with increasing flow rate, which could improve the model's fit to the experimental results.

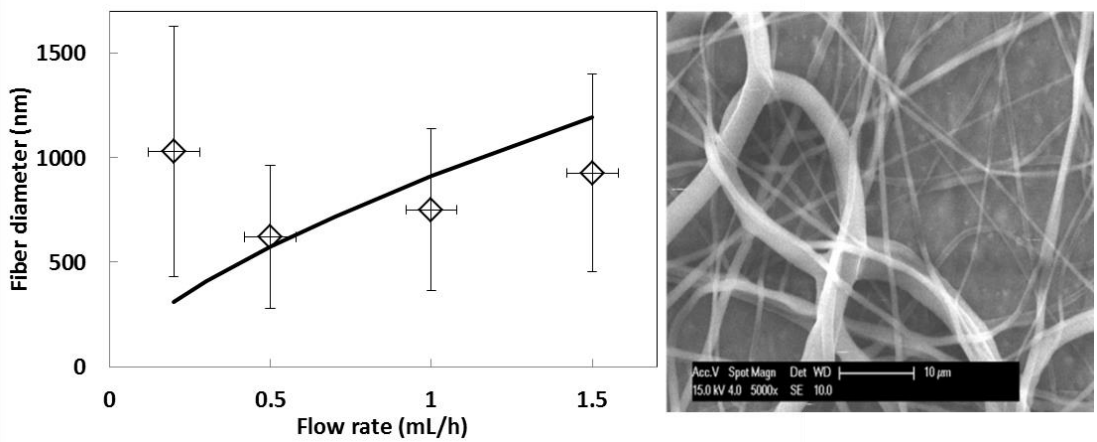

Fig. 6. Fiber diameter as a function of the flow rate (symbols) at a distance of 10 cm, 8 kV and a [PCL] of 20% (shown on the left). The terminal jet diameter theory (curve) was applied by modelling the current as 334 nA. Other model parameters used were $\gamma = 29.6$ dyn/cm, $\varepsilon = 1$ and $\chi = 12$. The SEM micrograph (on the right) displays the important variation in fiber diameter obtained at $Q = 0.2$ mL/h.

Overall, the general trends observed with the fiber diameter as a function of each of the studied parameters of polymer concentration, applied voltage, tip to collector distance and flow rate, are consistent with the observations made on other systems by other research groups, which are well summarized in a table format by Pham et al. (2006). In this paper, polymer concentration and applied voltage displayed the greatest impact on fiber diameter.

4. Conclusion

In this paper, the electrospinning of polycaprolactone nanofibers was optimized using a solvent mixture of tetrahydrofuran and methanol in a 3:1 ratio. The solvent choice was motivated by an exploration towards greener alternatives to the halogenated solvents most often used for electrospinning. The process was optimized for the production of smaller fibers with a narrower fiber diameter distribution by studying parameters such as polymer concentration, applied voltage, the tip to collector distance, and the solution flow rate. The experimental results were modelled using terminal jet diameter theory. The polymer concentration and the applied voltage showed the greatest influence on the fiber diameter. Process parameters were optimal for a 20% polycaprolactone concentration spun at a flow rate of 0.5 mL/h, with a tip to collector distance of 15 cm and an applied voltage of 8 kV. Fibers spun under these conditions resulted in diameters of 546 ± 173 nm.

Acknowledgements

Authors would like to thank the AUTO21 of the Ontario Centre of Excellence and the Academic Research Program of RMC for their financial support which made possible the research presented in this scientific research paper.

References

Baji A., Mai Y.-W., Wong S.-C., Abtahi M., Chen P. (2010). Electrospinning of polymer nanofibers: Effects on oriented morphology, structures and tensile properties. Composites Science and Technology, 70, 703-718.

Dzenis Y. (2004). Spinning continuous fibers for nanotechnology. Science, 304, 1917-1919.

Formhals A. (1934). Process and apparatus for preparing artificial threads, US patent no. 1975504.

Fridrikh S.V., Yu J.H., Brenner M.P., Rutledge G.C. (2003). Controlling the fiber diameter during electrospinning. Physical Review Letters, 90, 144502-1–144502-4.

Huczko A. (2000). Template-based synthesis of nanomaterials. Applied Physics A, 70, 365-376.

Luo C.J., Nangrejo M., Edirisinghe M. (2010). A novel method of selecting solvents for polymer electrospinning. Polymer, 51, 1654-1662.

Luo C.J., Stoyanov S.D., Stride E., Pelan E., Edirisinghe M. (2012). Electrospinning versus fibre production methods: From specifics to technological convergence. Chemical Society Reviews, 41, 4708-4735.

Luo C.J., Stride E., Edirisinghe M. (2012). Mapping the influence of solubility and dielectric constant on electrospinning polycaprolactone solutions. Macromolecules, 45, 4669-4680.

Nain A.S., Wong J., Amon C., Sitti M. (2006). Drawing suspended polymer micro-/nanofibers using glass micropipettes. Applied Physics Letters, 89, 183105-1–183105-3.

Pham Q.P., Sharma U., Mikos A.G. (2006). Electrospinning of polymeric nanofibers for tissue engineering applications: A review. Tissue Engineering, 12, 1197-1211.

Reneker D.H., Yarin A.L., Fong H., Sureeporn K. (2000). Bending instability of electrically charged liquid jets of polymer solutions in electrospinning. Journal of Applied Physics, 87, 4531-4547.

Reneker D.H., Yarin A.L., Zussman E., Xu H. (2007). Electrospinning of nanofibers from polymer solutions and melts. Advances in Applied Mechanics, 41, 44-195.

Subbiah T., Bhat G.S., Tock R.W., Parameswaran S., Ramkumar S.S. (2005). Electrospinning of nanofibers. Journal of Applied Polymer Science, 96, 557-569.

Taylor G. (1969). Electrically driven jets. Proceedings of the Royal Society of London A, 313, 453-475.

Thompson C.J., Chase G.G., Yarin A.L., Reneker D.H. (2007). Effects of parameters on nanofiber diameter determined from electrospinning model. Polymer, 48, 6913-6922.
Valavanidis A., Vlachogianni T. (2012). "Green Chemistry and Green Engineering" Synchrona Themata Publishing, 81-92.
Zoppe J.O., Peresin M.S., Habibi Y., Venditti R.A., Rojas O.J. (2009). Reinforcing poly(ε-caprolactone) nanofibers with cellulose nanocrystals. ACS Applied Materials & Interfaces, 1, 1996-2004.